

Spectrum of magnetic hyperfine fields at ^{111}Cd probe nuclei in the pseudobinary rare-earth Laves-phase compounds $R_{1-x}\text{Y}_x\text{Co}_2$

P. de la Presa,^{1,*} A. F. Pasquevich,² and M. Forker^{2,†}

¹*Helmholtz-Institut für Strahlen- und Kernphysik der Universität Bonn, Nussallee 14-16, D-53115 Bonn, Germany*

²*Departamento de Física, Facultad de Ciencias Exactas, Universidad Nacional de La Plata. 1900 La Plata and Comisión de Investigaciones Científicas de la Provincia de Buenos Aires, Argentina*

(Received 20 February 2005; revised manuscript received 1 August 2005; published 3 October 2005)

The spectrum of the magnetic hyperfine fields at the closed-shell probe nucleus ^{111}Cd on the rare earth (R) site of the pseudobinary Laves-phase compounds $R_{1-x}\text{Y}_x\text{Co}_2$ has been investigated by perturbed angular correlation (PAC) spectroscopy at 10 K for the rare earth $R=\text{Tb}$ and Ho at various Y concentrations $x\leq 0.8$ and for $R=\text{Gd}$, Dy , Er at the concentration $x=0.3$. Up to four components with different magnetic interaction frequencies ν_M^j could be resolved from the PAC spectra. The relative intensities of these components are in fair agreement with those of a binomial distribution of Y atoms on the four nearest neighbor (NN) R sites of the probe nucleus. For all R constituents, one finds a strictly linear relation between the number n_R of NN R atoms and the magnetic hyperfine frequencies: $\nu_M^j = \nu_M(4\text{Y}) + \Delta\nu_M \times n_R$. The frequency $\nu_M(4\text{Y}) = 35(2)$ MHz is independent of the R constituent and of the Y concentration up to $x\leq 0.6$. These properties identify $\nu_M(4\text{Y})$ as the contribution of the $\text{Co } 3d$ moments to the hyperfine interaction at the ^{111}Cd site. The frequency steps $\Delta\nu_M[\leq 0.1\nu_M(4\text{Y})]$ reflect the spin polarization directly induced by the $4f$ spins at the probe nucleus. From Gd to Er , the spin polarization decreases much stronger than expected from the linear variation of the $4f$ spin in the heavy R series. An indirect $4f$ contribution caused by a dependence of the $\text{Co } 3d$ moment on the number of R neighbors can be excluded. The relation $\nu_M^j = \nu_M(4\text{Y}) + \Delta\nu_M \times n_R$ then implies that the contributions of the $3d$ and $4f$ spins to the magnetic hyperfine field in $R\text{Co}_2$ have the same relative sign.

DOI: 10.1103/PhysRevB.72.134402

PACS number(s): 75.30.-m, 76.80.+y, 76.60.Jx, 75.50.-y

I. INTRODUCTION

The magnetic properties of intermetallic compounds of $3d$ - and $4f$ -elements R_xM_y (R =rare earth, M =Fe, Co, Ni, Mn) have been intensively investigated by measurements of the magnetic hyperfine field B_{hf} experienced by the nuclei of suitable probe atoms.^{1,2} The magnetic hyperfine field at the nuclei of nonrare earth atoms is caused by the Fermi contact term in the nucleus-electron interaction and reflects the spin polarization of the s electrons at the probe nucleus. A finite s -electron spin density may arise from the spin polarization of the host conduction electrons, the polarization of the electron core of the probe by a localized spin, and the overlap of the valence electrons of the probe with spin polarized valence electrons of the magnetic ions.

In R_xM_y compounds where the transition element carries a $3d$ -magnetic moment, both the $3d$ and the $4f$ sublattice contribute to the hyperfine field. One way to separate these contributions and study the $3d$ - $4f$ interaction is the systematic variation of the $4f$ contribution by partial substitution of the magnetic R atoms by nonmagnetic La, Y, or Lu. In the present paper we report a perturbed angular correlation (PAC) study of the spectrum of magnetic hyperfine fields at the probe nucleus ^{111}Cd on the R site of pseudobinary $R_{1-x}\text{Y}_x\text{Co}_2$ which is an extension of our previous investigation of the $4f$ -spin dependence of $B_{\text{hf}}(^{111}\text{Cd})$ in $R\text{Co}_2$ (Ref. 3).

The magnetic properties of $R\text{Co}_2$ depend crucially on the interaction of the $3d$ and the $4f$ sublattices. The enhanced Pauli paramagnet YCo_2 shows a metamagnetic transition to a highly magnetized state in external magnetic fields

$B_{\text{cr}} > 80$ T, indicating that the $\text{Co } 3d$ band in YCo_2 is on the verge of spontaneous magnetic order. In $R\text{Co}_2$, intra-atomic $4f$ - $5d$ and interatomic $5d$ - $3d$ exchange spin polarizes the itinerant $3d$ -electron system, resulting in magnetic order with Curie temperatures $T_C \leq 392$ K (GdCo_2) when the corresponding molecular field B_{mol} exceeds the critical value of 80 T (Refs. 4 and 5).

The interaction of the $3d$ and $4f$ sublattice in $R\text{Co}_2$ has been previously investigated by ^{59}Co (Refs. 6–9), ^{165}Ho (Refs. 10 and 11), and ^{159}Tb (Ref. 12) measurements of the hyperfine field distribution in $R_{1-x}\text{Y}_x\text{Co}_2$. The NMR spectra show a satellite structure caused by the statistical occupation of the nearest neighbor (NN) R sites of the NMR nuclei by nonmagnetic Y. The dominant contribution to the total hyperfine field comes in these cases from the electronic shell of the probe nucleus itself. The hyperfine field of ^{59}Co in $R\text{Co}_2$ mainly stems from the core polarization by the $\text{Co } 3d$ moment and has a substantial anisotropic orbital contribution, the field at ^{165}Ho is dominated by the large unquenched orbital angular momentum of the $4f$ shell. The extraction of the environmental contributions to the hyperfine field distributions in the presence of strong probe-related effects is a complex task, and it appears interesting to extend these substitution experiments to closed-shell probes where the s -electron spin polarization induced by the host moments is the only source of the magnetic hyperfine interaction. We have investigated the spectrum of hyperfine fields experienced by the closed-shell probe ^{111}Cd in $\text{Tb}_{1-x}\text{Y}_x\text{Co}_2$ at 10 K as a function of the Y concentration in the range $0 \leq x \leq 0.8$. Furthermore,

$\text{Ho}_{1-x}\text{Y}_x\text{Co}_2$ was studied in the concentration range $0 \leq x \leq 0.5$. PAC measurements were also carried out for the R constituents $R=\text{Gd}$, Dy , and Er at the Y concentration $x=0.3$.

II. EXPERIMENTAL DETAILS

A. Sample preparation and equipment

The PAC measurements were carried out with the 171–245 keV cascade of ^{111}Cd which is populated by the electron capture decay of the 2.8 d isotope ^{111}In . The samples were produced by arc melting of the metallic components in the stoichiometric ratio in an argon atmosphere and characterized by x-ray diffraction. Most compounds were single C15 phases. Although the samples were remelted several times for homogenization, a slight contamination by a foreign phase, possibly YCo_3 , was observed in a few cases. The relative intensity of this foreign phase was usually $\leq 5\%$.

The samples were doped with the PAC probe $^{111}\text{In}/^{111}\text{Cd}$ by diffusion (800 °C, 12 h) of carrier-free ^{111}In into the host lattices. Annealing for longer periods (up to eight days) systematically leads to a deterioration of the PAC spectra. We therefore refrained from other heat treatment than the diffusion. PAC measurements were carried out with a standard four-detector BaF_2 setup. The samples were cooled to 10 K in a closed-cycle He refrigerator.

B. Data analysis

The angular correlation theory of two successive γ rays of a γ - γ cascade, expressed by angular correlation coefficients A_{kk} ($k=2,4$) may be modulated in time by hyperfine interactions (HFI's) in the intermediate state of the cascade. For polycrystalline samples this modulation can be described by the perturbation factor $G_{kk}(t)$ which depends on the multipole order, the symmetry and time dependence of the interaction, and on the spin of the intermediate state (for details see, e.g., Frauenfelder and Steffen¹³).

The absence of an electric quadrupole at ^{111}Cd in paramagnetic $R\text{Co}_2$ (Ref. 3) shows that the probe atom resides on the cubic R site. In the ferromagnetic phase we are therefore dealing with a perturbation by a pure magnetic interaction, characterized by the Larmor frequency $\omega_m = 2\pi\nu_m = g\mu_N B_{\text{hf}}/\hbar$. In this case the perturbation factor can be expressed in an analytical form

$$G_{22}(t) = 1/5 + 2/5 \sum_{n=1,2} \cos(n\omega_m t). \quad (1)$$

If the ensemble of the probe nuclei is subject to a distribution rather than a unique hyperfine interaction, the nuclear spins of the ensemble no longer precess all with the same frequency and an attenuation of the oscillation amplitudes results which is the stronger the broader the distribution. The effect of a Lorentzian HFI distribution of relative width δ on the angular correlation can be approximated by

$$G_{kk}(t) = s_{k0} + \sum_n s_{kn} \cos(\omega_n t) \exp(-\delta n \omega_n t). \quad (2)$$

When several fractions of nuclei subject to different HFI's are found in the same sample, the effective perturbation factor is given by

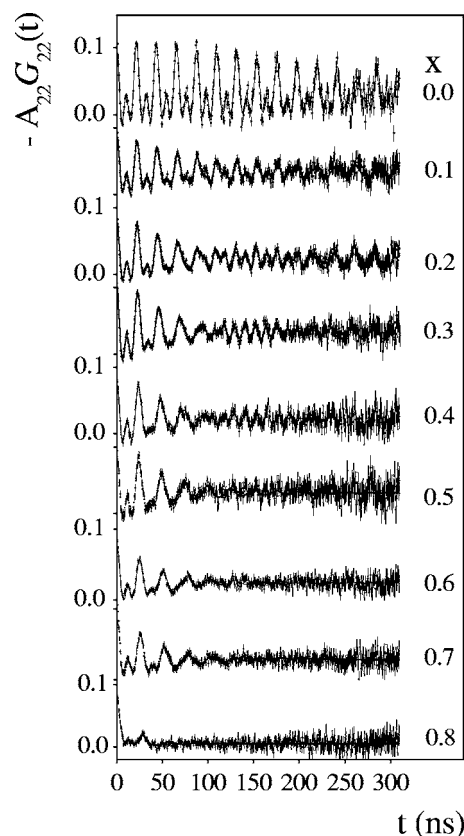


FIG. 1. PAC spectra of ^{111}Cd in $\text{Tb}_{1-x}\text{Y}_x\text{Co}_2$ at 10 K for different Y concentrations.

$$G_{kk}(t) = \sum_i f_i G_{kk}^i(t), \quad (3)$$

f_i (with $\sum_i f_i = 1$) is the relative intensity of the i th fraction.

III. MEASUREMENTS AND RESULTS

In all compounds $R_{1-x}\text{Y}_x\text{Co}_2$ a PAC spectrum was taken in the paramagnetic phase at room temperature. Without exception, the angular correlation was found to be as unperturbed as in $R\text{Co}_2$ (Ref. 3) from which we can conclude that at all Y concentrations and R constituents of $R_{1-x}\text{Y}_x\text{Co}_2$ the probe ^{111}Cd resides on the cubic R site.

The PAC spectra of ^{111}Cd in $\text{Tb}_{1-x}\text{Y}_x\text{Co}_2$ at 10 K for the Y concentrations $0 \leq x \leq 0.8$ are shown in Fig. 1. The periodic modulation of the anisotropy in TbCo_2 ($x=0.0$) is characteristic for a perturbation by a single magnetic hyperfine interaction. The Lorentzian distribution of the hyperfine field responsible for the weak damping of oscillation amplitudes has a relative width of $\delta \leq 0.01$ [see Eq. (2)]. As Y is added to TbCo_2 , the periodicity is lost, the oscillation amplitudes decay with increasing time. At small and intermediate concentrations $0.1 \leq x \leq 0.5$ one observes a complex modulation pattern at times $t > 100$ ns which is clear evidence for a superposition of several components with different, well-defined magnetic hyperfine frequencies ν_M^i . These modulations disappear for larger concentrations $x > 0.5$.

For concentrations $x \leq 0.5$, up to four discrete components with relative intensities f_i and well-defined frequencies ν_M^i

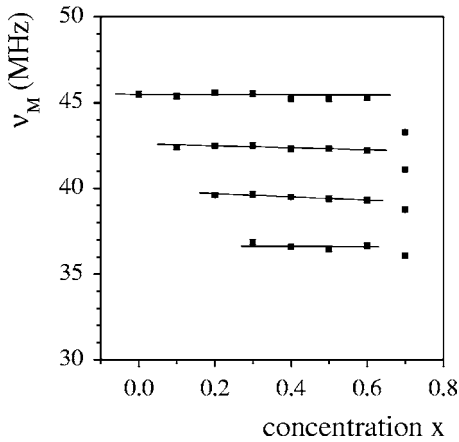


FIG. 2. Four magnetic interaction frequencies ν_M^j derived from the PAC spectra of ^{111}Cd in $\text{Tb}_{1-x}\text{Y}_x\text{Co}_2$ as a function of the Y concentration x .

are necessary to describe the measured perturbation factor. At these concentrations the linewidths could be treated as free parameters and the analysis resulted in $\delta_i \leq 0.03$. Starting at the highest ν_M , the frequencies decrease in constant steps of $\Delta\nu_M = 2.9(1)$ MHz.

At higher concentrations $x > 0.5$, when the perturbation factor loses its complex oscillatory structure at $t > 100$ ns, the spectra can in principle be reproduced by a single site subject to a broad hyperfine field distribution ($\delta \sim 0.1$). However, to come to a consistent description of the spectra over the entire concentration range, we assumed several well-defined hyperfine interactions also for large Y concentrations. In this case it becomes necessary to constrain the Lorentzian line widths δ_i in the analysis. It was assumed that the same values of δ_i hold for all concentrations and the measurements were then analyzed by fitting a superposition of several components with relative intensities f_i , hyperfine frequencies ν_M^j , and fixed linewidths $\delta_i = 0.03$ [see Eqs. (2) and (3)] to the experimental spectra.

At $x = 0.1$ and $x = 0.2$ two and three components, respectively, were sufficient to describe the measured spectra. For $x \geq 0.3$, four different components, all of them with a Lorentzian line-width of $\delta_i = 0.03$, were adjusted to the measured perturbation factor. To test for a correlation between the frequencies and the relative intensities, generally two fits were carried out. First, the intensities were fixed to the values expected for a binomial distribution of $n_R = 4$ to 0 R atoms on the four nearest neighbor R sites of the probe, assuming that the hyperfine frequencies decrease with decreasing number of NN R atoms which is suggested by the fact that the frequency of the strongest component at $x \leq 0.2$ is identical to that measured in $R\text{Co}_2$. In the second step of the analysis, the intensities were treated as free fit parameters. The assumptions on the relative intensities were found to affect the frequencies by less than 0.5%. The frequencies ν_M^j and the relative intensities f_i of the components derived from the measured spectra at different concentrations are collected in Figs. 2 and 3.

In addition to $\text{Tb}_{1-x}\text{Y}_x\text{Co}_2$, PAC spectra were measured for all other heavy R at the concentration $x = 0.3$. This par-

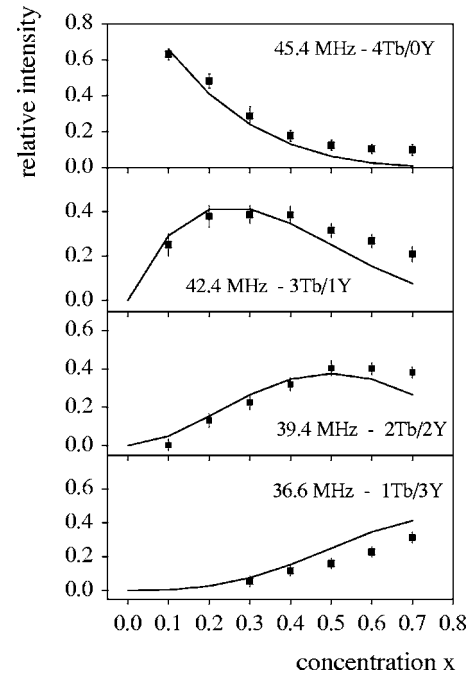


FIG. 3. Relative intensities of the four components with frequencies ν_M^j as a function of the Y concentration x , derived from the PAC spectra ^{111}Cd in $\text{Tb}_{1-x}\text{Y}_x\text{Co}_2$ at 10 K, with the relative widths of the Lorentzian frequency distributions fixed to $\delta_i = 0.03$. The solid lines correspond to the probabilities of finding $n_R = 4, 3, 2, 1$ R atoms on the four nearest neighbor R sites of the probe nucleus for the case of a binomial distribution.

ticular concentration was chosen because in the series $\text{Tb}_{1-x}\text{Y}_x\text{Co}_2$ the four magnetic configurations could be separated with the highest precision at $x \approx 0.3-0.4$. In the case of $R = \text{Ho}$, the measurements were extended to other concentrations.

The PAC spectra observed at the concentration $x = 0.3$ for the constituents $R = \text{Gd}, \text{Tb}, \text{Dy}, \text{Ho}$, and Er are compared in Fig. 4. One may distinguish two groups: The spectra of $\text{Gd}_{0.7}\text{Y}_{0.3}\text{Co}_2$ and $\text{Tb}_{0.7}\text{Y}_{0.3}\text{Co}_2$ are characterized by a complex oscillatory structure at large delay times, those of $R = \text{Dy}, \text{Ho}, \text{Er}$ only show a decay of the oscillation amplitudes. Similar magnetic perturbation patterns were found in $\text{Ho}_{1-x}\text{Y}_x\text{Co}_2$ up to Y concentrations $x \leq 0.4$. At higher concentrations the magnetic interaction disappeared and the spectra reflected broad, temperature-independent quadrupole distributions. The observation of damped amplitudes rather than a complex oscillatory structure implies that for $R = \text{Dy}, \text{Ho}, \text{Er}$ the frequency differences of the components are much smaller than for $R = \text{Gd}$ and Tb .

In the case of $\text{Gd}_{0.7}\text{Y}_{0.3}\text{Co}_2$ the analysis resulted in four components with sharply defined magnetic interactions, decreasing from the largest value $\nu_M = 50.5(1)$ MHz in constant steps of $\Delta\nu_M = 3.98(5)$ MHz. This large $\Delta\nu_M$ allowed the determination of the Lorentzian line-widths δ_i without constraints. For all four components we obtained $\delta_i \leq 0.015$. The relative intensities f_i were comparable to those of $\text{Tb}_{0.7}\text{Y}_{0.3}\text{Co}_2$ shown in Fig. 3.

The spectra showing a damping of the oscillation amplitudes, i.e., those observed in $R_{0.7}\text{Y}_{0.3}\text{Co}_2$; $R = \text{Dy}, \text{Er}$, and

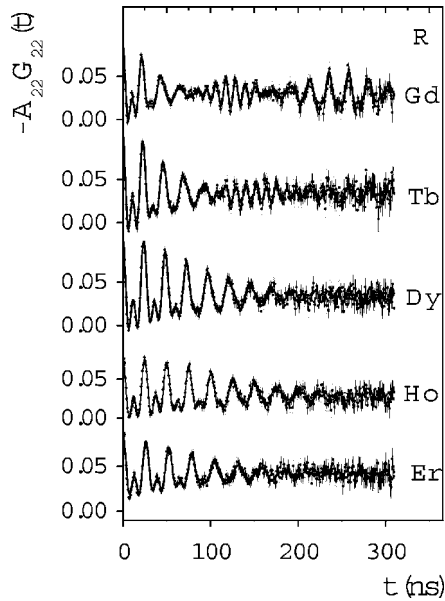


FIG. 4. PAC spectra of ^{111}Cd in $R_{0.7}\text{Y}_{0.3}\text{Co}_2$ at 10 K for $R = \text{Gd}, \text{Tb}, \text{Dy}, \text{Ho}, \text{Er}$.

$\text{Ho}_{1-x}\text{Y}_x\text{Co}_2$; $x \leq 0.4$ were analyzed constraining the Lorentzian widths to $\delta_i = 0.03$. Fits assuming (i) three or four components with free intensities, and (ii) four components with the intensities fixed to the values for a binomial distribution of Y atoms were compared. The assumption of four components (for $x = 0.3$ and 0.4) resulted in clearly better fits. Using either free or fixed intensities left the frequencies of $R_{0.7}\text{Y}_{0.3}\text{Co}_2$ unchanged within a range of one percent. In the case of $\text{Ho}_{1-x}\text{Y}_x\text{Co}_2$, the variation of the frequencies ν_M^j with the Y concentration was found to be ≤ 0.7 MHz ($\leq 2\%$) for $0.1 \leq x \leq 0.5$. The frequencies ν_M^j obtained in this way from the spectra $R_{0.7}\text{Y}_{0.3}\text{Co}_2$; $R = \text{Dy}, \text{Er}$, and $\text{Ho}_{1-x}\text{Y}_x\text{Co}_2$; $x \leq 0.4$ differ by multiples of a constant $\Delta\nu_M$. The frequency step, however, is considerably smaller than in the case of $\text{Tb}_{1-x}\text{Y}_x\text{Co}_2$ and $\text{Gd}_{0.7}\text{Y}_{0.3}\text{Co}_2$. This is clearly seen in Fig. 5 where the frequencies ν_M^j derived from the spectra of $R_{0.7}\text{Y}_{0.3}\text{Co}_2$ for the different R constituents have been collected. The frequencies shown for Tb and Ho correspond to the average values of the concentration ranges $0 \leq x \leq 0.6$ and $0 \leq x \leq 0.4$, respectively.

IV. DISCUSSION

The main results of the low temperature PAC measurements displayed in Figs. 2, 3, and 5 can be summarized as follows:

(1) Up to four different magnetic configurations with frequencies ν_M^j and relative intensities f_i have been identified in the PAC spectra of $R_{1-x}\text{Y}_x\text{Co}_2$ ($R = \text{Tb}, \text{Ho}$) and $R_{0.7}\text{Y}_{0.3}\text{Co}_2$ ($R = \text{Gd}, \text{Dy}, \text{Er}$). The low-concentration spectra of $R = \text{Gd}, \text{Tb}$ leave no doubt that these frequencies are sharply defined. The relative width of the field distribution does not exceed $\delta = 0.03$.

(2) The frequencies ν_M^j differ by multiples of a constant frequency step $\Delta\nu_M$ which strongly decreases from Gd to Er.

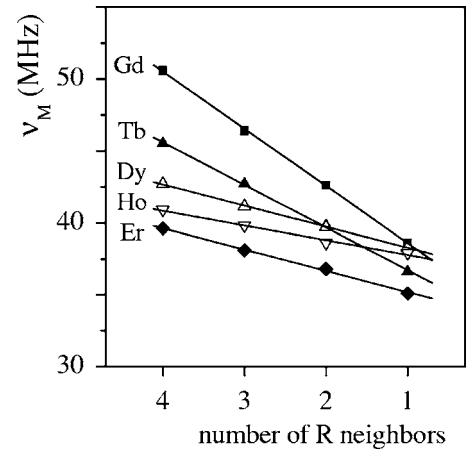


FIG. 5. Frequencies ν_M^j detected in the PAC spectra of $^{111}\text{Cd}:R_{1-x}\text{Y}_x\text{Co}_2$ versus the number of R atoms in the NN R shell of the probe nucleus. The frequencies shown for $R = \text{Tb}$ and Ho are the average values of the concentration ranges $0 \leq x \leq 0.6$ and $0 \leq x \leq 0.4$, respectively. The frequencies for the other R constituent correspond to the Y concentration $x = 0.3$.

(3) The Y content can be increased to considerable levels without affecting the frequencies. In $\text{Tb}_{1-x}\text{Y}_x\text{Co}_2$ and $\text{Ho}_{1-x}\text{Y}_x\text{Co}_2$ the frequencies are practically independent of the Y concentration up to $x \leq 0.6$ (Tb) and 0.4 (Ho). In this concentration range, the largest of the four frequencies (~ 45 MHz) of $\text{Tb}_{1-x}\text{Y}_x\text{Co}_2$ decreases (see Fig. 2) by less than 0.05 MHz (0.1%), the second and third largest frequencies by at most 0.5 MHz.

(4) For concentrations $x < 0.5$, the relative intensities of the four fractions in the spectra of $\text{Tb}_{1-x}\text{Y}_x\text{Co}_2$ agree well with the probabilities of finding $n_R = 4, 3, 2, 1$ R atoms on the 4 NN R sites of the probe nucleus ^{111}Cd for the case of a random distribution (solid lines in Fig. 3). For $x > 0.5$, the relative intensities deviate slightly from the binomial probabilities suggesting some preference of the probe atom for the configurations with two or more Tb atoms.

The agreement between the measured intensities and the binomial probabilities identifies the number n_R of nearest R neighbors as the parameter which characterizes the four magnetic configurations detected in the PAC spectra. The observation of constant frequency steps then leads to the conclusion that the hyperfine interaction of ^{111}Cd on the R site of $R_{1-x}\text{Y}_x\text{Co}_2$ is a strictly linear function of the number n_R of nearest R neighbors. For all R constituents, the largest of the four frequencies is—within 1%—identical to that of ^{111}Cd in nondiluted $R\text{Co}_2$ (Ref. 3) which defines the point $n_R = 4$ on the n_R axis in Fig. 5.

We may therefore write the frequencies ν_M^j as

$$\nu_M^j = \nu_M(4Y) + \Delta\nu_M \times n_R. \quad (4)$$

The values of $\Delta\nu_M$ and $\nu_M(4Y)$ for the heavy rare earths derived from the data in Fig. 5 are plotted in Fig. 6 versus the R spin projection $(g-1)J$.

A decrease of the magnetic interaction upon substitution of R by Y atoms has also been found in NMR (Refs. 6–9) measurements of ^{59}Co in $R_{1-x}\text{Y}_x\text{Co}_2$ and ^{165}Ho in

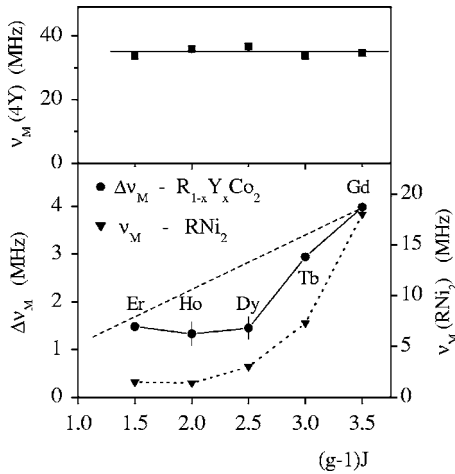


FIG. 6. Parameters $\nu_M(4Y)$ (top section) and $\Delta\nu_M$ (bottom section) describing the dependence of the magnetic frequencies ν_M^i of $^{111}\text{Cd}:R_{1-x}Y_x\text{Co}_2$ on the number n_R of nearest R neighbors of the probe nucleus versus the spin projection $(g-1)J$. $\nu_M(4Y)$ and $\Delta\nu_M$ were determined by fitting Eq. (4) to the data in Fig. 5. The dashed line illustrates a linear spin dependence of $\Delta\nu_M$. In addition, the bottom section also shows the spin dependence of the magnetic hyperfine frequency of ^{111}Cd in RNi_2 (right-hand scale).

$\text{Ho}_{0.03}\text{Gd}_x\text{Y}_{0.97-x}\text{Co}_2$ (Refs. 10 and 11) where the addition of Y leads to satellites at lower frequencies. Correspondingly, the addition of Gd to YFe_2 produces satellites at higher frequencies in the ^{89}Y NMR spectra of $\text{Y}_{1-x}\text{Gd}_x\text{Fe}_2$ (Refs. 14 and 15).

It is interesting to compare the ^{111}Cd PAC results displayed in Figs. 2 and 5 to those obtained by NMR for ^{165}Ho in $\text{Gd}_{0.97-x}\text{Ho}_{0.03}\text{Y}_x\text{Co}_2$ (Refs. 10 and 11). In both cases, discrete frequencies ν_M^i are observed which (for constant x) differ by constant frequency steps. For $R=\text{Gd}$ and the Y concentration $x=0.3$, the corresponding transferred hyperfine fields per NN Gd atom are 3.2 and 1.7 T at ^{165}Ho and ^{111}Cd , respectively. The PAC and the NMR results differ considerably with respect to the concentration dependence of ν_M^i . In the case of ^{165}Ho , the hyperfine field for a given n_R decreases monotonically with increasing Y concentration by as much as 2.5 T in the range $0 \leq x \leq 0.5$, in the case of ^{111}Cd the largest decrease in the same concentration range compatible with the experimental data in Fig. 2 is 0.2 T. When comparing these probes, it must be remembered that the huge hyperfine field at ^{165}Ho in $\text{Gd}_{0.97}\text{Ho}_{0.03}\text{Co}_2$ of ~ 743 T (free Ho^{3+} value: 808 T) is mainly caused by the orbital angular momentum of the $4f$ shell. Arif and McCausland,¹⁰ have pointed out that incipient quenching of the Ho moment by crystal field interactions which reduces the hyperfine field is expected to become more important when the exchange interaction is weakened by Y substitution and could thus account for the observed decrease of the hyperfine field with increasing Y content.

When discussing the frequency differences of the various components expressed by Eq. (4), the contribution of the dipolar field to the total hyperfine field has to be considered. The dipolar field seen by a probe nucleus on the cubic R site of the C15 lattice of $R\text{Co}_2$ ($n_R=4$) vanishes, but finite contributions B_{dip} are expected when the cubic symmetry is broken

by substituting up to three of the four NN R atoms by non-magnetic Y ($1 \leq n_R \leq 3$). Consequently, for a given value of n_R , the ensemble of probe nuclei is subject to field distribution rather than a unique hyperfine field. For random substitution, however, the ensemble average for each n_R still has cubic symmetry and the weighted sum over all dipolar contributions therefore vanishes, independent of the easy-magnetization direction. The corresponding frequency distributions are therefore centered at ν_M^i . Their width may be estimated from the dipolar field caused by a magnetic moment of $10 \mu_B$ at a distance of $(3/16)^{1/2}a$ (a = lattice constant of $R\text{Co}_2=0.72$ nm): $B_{\text{dip}} < 0.6$ T. For ^{111}Cd this corresponds to $\nu_M^{\text{dip}} < 1.5$ MHz, so that $\nu_M^{\text{dip}}/\nu_M^i \sim 3.5 \cdot 10^{-2}$. Such a narrow field distribution only causes a slow decay of the precession amplitudes with time. We may therefore conclude that the dipolar field does not contribute to the frequencies ν_M^i . The linear decrease of ν_M^i with decreasing number n_R reflects changes of the spin polarization at the probe site with the number of NN $4f$ spins.

According to Eq. (4), the hyperfine field consists of a local part $B_{\text{hf}}^{\text{loc}} \propto \Delta\nu_M n_R$ controlled by the nearest R neighbors and a contribution $\nu_M(4Y)$ from the “magnetic background” acting on the probe nuclei when the four nearest magnetic R neighbors have been substituted by non-magnetic Y atoms.

Remarkably, the “background” contribution $\nu_M(4Y)$ is to a large degree independent of the R constituent and of the Y concentration: At $x=0.3$, the mean value of all R constituents is $\nu_M(4Y)=35(2)$ MHz with a standard deviation of 5% (see Fig. 6), and for $R=\text{Tb}$ and Ho where several concentrations have been investigated, this value remains unchanged up to Y concentrations of $x \leq 0.6$ (Tb) and $x \leq 0.4$ (Ho).

The absence of a R dependence of $\nu_M(4Y)$ implies that contributions to the hyperfine field from $4f$ spins in the second NN shell at distance $a/\sqrt{2}$ ($a=7.2$ Å) and beyond are negligibly small which favors short-range $4f-5d$ exchange and $5d$ -probe overlap¹⁶ rather than long-range Ruderman-Kittel-Kasuya-Yosida (RKKY) coupling as the mechanism leading to the spin polarization at the probe nucleus.

The frequency $\nu_M(4Y)$ therefore reflects the s -electron spin polarization caused at the probe site by the Co sublattice. The dominant contribution is expected to come from the 12 nearest Co neighbors of the probe at $0.414 a$. Each of these 12 Co sites is surrounded by 6 R positions. One of these R sites is occupied by the probe itself, two are nearest R neighbors to the probe occupied by Y atoms and on the remaining three in the second and third NN R shells of the probe one has—depending on the Y concentration—a statistical distribution of R and Y atoms.

The observation that $\nu_M(4Y)$ in $\text{Tb}_{1-x}\text{Y}_x\text{Co}_2$ and $\text{Ho}_{1-x}\text{Y}_x\text{Co}_2$ is independent of the degree of Y substitution up to concentrations of $x \leq 0.6$ (Tb) and $x \leq 0.4$ (Ho) then leads us to conclude that the average $3d$ moment of these 12 NN Co atoms is constant over a large concentration range. This conclusion is consistent with the saturation behavior of the Co $3d$ moment: Above the critical field B_{cr} for the metamagnetic transition, the Co $3d$ moment varies—if at all—only slightly with increasing molecular field B_{mol} (Ref. 4). For a quantitative discussion, we consider the concentration dependence of the molecular field B_{mol} acting at the nearest Co

neighbors of the probe. As the $3d-4f$ interaction is of short range, it appears justified to assume that B_{mol} is proportional to the number of nearest R neighbors $n_R(\text{Co})$ of these Co atoms: $B_{\text{mol}} \propto n_R(\text{Co})$. [Note: We use the notations n_R and $n_R(\text{Co})$ to describe the number of NN R atoms of the probe (R) site and of the Co sites, respectively]. Assuming that for a given NN R environment of the probe, characterized by n_R , the three R atoms in the second and third R shell of the probe are statistically substituted by Y, the average number of NN R atoms $n_R(\text{Co})$ surrounding the NN Co sites of the probe varies with the Y concentration x as

$$n_R(\text{Co}) = n_R/2 + 3(1-x). \quad (5)$$

The first term comes from the two R sites which are nearest neighbors both to the probe and the Co site under consideration, the second term accounts for the other three R sites.

With $B_{\text{mol}} \propto n_R(\text{Co})$ and Eq. (5) one may estimate the critical concentration x_{cr} at which the molecular field drops below $B_{\text{cr}} \approx 80$ T. The molecular field of $R\text{Co}_2$ [$n_R(\text{Co})=6$] is about 250 and 380 T for $R=\text{Ho}$ and Tb , respectively (Ref. 4). For $n_R=0$, the decrease of B_{mol} with increasing x reaches B_{cr} at $x_{\text{cr}} \sim 0.6$ and 0.36 for Tb and Ho , respectively. These values agree fairly well with the concentration ranges for which our data indicate a constant $3d$ moment. Our data are also in agreement with the result of a neutron diffraction study of $\text{Tb}_{1-x}\text{Y}_x\text{Co}_2$ (Ref. 17) where a substantial decrease of the $3d$ moment from $\mu_{\text{Co}} \approx 1 \mu_B$ was observed only for $x > 0.6$. A similar conclusion has been drawn from the ^{159}Tb NMR data (Ref. 12).

With $\nu_M(4Y)$ independent of R , the entire contribution of the $4f$ sublattice to the hyperfine field B_{hf}^{4f} is described by the local part $B_{\text{hf}}^{\text{loc}} \propto \Delta\nu_M n_R$. In principle, two $4f$ contributions are conceivable: a direct contribution of the NN $4f$ spins to the spin polarization at the probe and an indirect $4f$ contribution caused by a dependence of the $3d$ moment on the number n_R via changes of the local molecular field B_{mol} .

The observation that the frequencies ν_M^j are practically independent of the Y concentration up large values of x , however, argues strongly against an indirect $4f$ contribution to $B_{\text{hf}}^{\text{loc}}$. As shown by Eq. (5), both the number n_R of NN R atoms and the Y concentration x affect the molecular field at the 12 nearest Co neighbors of the probe. If the $3d$ moment of this Co environment would change with n_R via B_{mol} , the same mechanism should lead to a variation of the $3d$ moment with the Y concentration. This should show up as a concentration dependence of the frequencies ν_M^j in the PAC spectra (see Fig. 2) since for a given n_R the direct $4f$ contribution can be assumed to be constant.

Consider the case of $\text{Tb}_{1-x}\text{Y}_x\text{Co}_2$: Even the smallest of the four frequencies ($\nu_M=37$ MHz, see Fig. 2), which corresponds to $n_R=1$, is practically constant up to $x \leq 0.6$. This means that the molecular field in $\text{Tb}_{1-x}\text{Y}_x\text{Co}_2$ can be reduced by changes of the Y concentration to about $B_{\text{mol}} \sim 110$ T [Eq. (5) with $n_R=1$, $x=0.6$] without affecting the $3d$ moment. Consequently, there is no support for a change of the moment with increasing n_R , where $B_{\text{mol}} > 110$ T.

Based on these arguments, we exclude—for the Y concentrations studied in this paper—a sizeable indirect $4f$ contri-

bution to the discrete frequency steps $\Delta\nu_M$ via changes of the local $3d$ moment. This conclusion is also supported by the fact the frequencies ν_M^j are sharply defined. If the $3d$ moments would vary with the number $n_R(\text{Co})$, one would expect distributions of the interaction frequencies because of the statistical occupation of the NN R sites of the Co sites with R and Y atoms.

In the analysis of ^{59}Co NMR spectra of $\text{Y}_{1-x}\text{R}_x\text{Co}_2$, Hiro-sawa *et al.*,⁶ and Hiro-sawa and Nakamura^{7,8} arrive at a different result. The appearance of satellites at lower frequencies when R atoms are substituted by Y atoms is attributed to a strong dependence of the Co moment on the number $n_R(\text{Co})$ of nearest R neighbors.

The contributions of the $3d$ and the $4f$ sublattice to the total hyperfine field of ^{111}Cd in $\text{R}_{1-y}\text{Y}_y\text{Co}_2$ are now clearly identified: The linear increase of the hyperfine field with increasing n_R reflects the spin polarization induced by the nearest $4f$ spins at the probe site: $B_{\text{hf}}^{4f} = B_{\text{hf}}^{\text{loc}} \propto \Delta\nu_M n_R$, and $\nu_M(4Y)$ describes the contribution of the $3d$ system $B_{\text{hf}}^{3d} \propto \nu_M(4Y)$.

The observation that the frequencies ν_M^j increase with increasing number of nearest R neighbors [Fig. 5 and Eq. (4)] then implies that the $3d$ and the $4f$ contribution to the total hyperfine field have the same relative sign: $B_{\text{hf}} = B_{\text{hf}}^{3d} + B_{\text{hf}}^{4f}$. The assumption of an opposite sign, $B_{\text{hf}} = B_{\text{hf}}^{3d} - B_{\text{hf}}^{4f}$ is in conflict with the experimental observation: If one accepts that B_{hf}^{4f} decreases with decreasing number n_R of nearest R neighbors, an explanation of $\nu_M^j = \nu_M(4Y) + \Delta\nu_M \times n_R$ with the assumption $B_{\text{hf}} = B_{\text{hf}}^{3d} - B_{\text{hf}}^{4f}$ would require that the $3d$ contribution and thus the $3d$ moment also decreases with decreasing n_R . This, however, is incompatible [see Eq. (5)] with the fact that the individual frequencies ν_M^j are constant over a large range of Y concentrations.

Our conclusion that the relative sign the $3d$ and the $4f$ contributions to B_{hf} is positive agrees with the analysis of the satellite structure of ^{59}Y NMR spectra in pseudobinary $\text{Gd}_x\text{Y}_{1-x}\text{Fe}_2$ (Refs. 14 and 15). A NN Gd atom increases the hyperfine field at the Y site of YFe_2 . First-principles electronic-structure calculations by Guenzburger *et al.*¹⁸ have shown that the transferred hyperfine field responsible for this increase arises from the direct polarization of the s electrons at Y by the $4f$ spin of Gd. The larger B_{hf} in the presence of a NN R atom then implies that the $3d$ and the $4f$ contributions to B_{hf} have the same direction. From NMR spectra of ^{165}Ho in $\text{Gd}_{0.97-x}\text{Ho}_{0.03}\text{Y}_x\text{Co}_2$ also Arif *et al.*¹¹ conclude that the NN $4f$ and the $3d$ contributions to B_{hf} have the same relative sign.

In R metals and many R intermetallic compounds in which magnetic order is sustained by indirect $4f-4f$ interaction alone, the hyperfine field induced by the localized $4f$ spins at the nucleus of a nonmagnetic probe atom is in first approximation proportional to the effective exchange parameter Γ and the spin projection $(g-1)J$. As Γ varies little with the atomic number of the heavy R , one mostly finds a more or less linear dependence of B_{hf} on the R spin projection. It has been shown above, that the frequency steps $\Delta\nu_M$ [Eq. (4) and Figs. 2 and 4] reflect the conduction-electron polarization (CEP) directly induced at ^{111}Cd by the NN $4f$ spins and therefore one would expect an approximately linear decrease of $\Delta\nu_M$ from Gd to Er. Figure 6, however, shows that the

spin dependence of $\Delta\nu_M$ is far from linear. Especially in the case of $R=\text{Dy}$ and Ho , $\Delta\nu_M$ is about a factor of 2 smaller than expected.

This pronounced nonlinearity of $\Delta\nu_M$ versus $(g-1)J$ has a striking resemblance to the spin dependence of the hyperfine field of ^{111}Cd in the isostructural series RNi_2 (Ref. 19). In RNi_2 , the $3d$ element carries a magnetic moment of at most a few hundredths of a Bohr magneton. The conduction electron polarization in RNi_2 is therefore exclusively due to the indirect $4f-4f$ interaction. The s -electron density and the lattice parameters of RCO_2 and RNi_2 are rather similar and if we presume the same for the exchange parameter, the $4f$ contribution to the total hyperfine field of ^{111}Cd in RCO_2 should be of the order of the hyperfine field of ^{111}Cd in RNi_2 . The comparison of $\Delta\nu_M$ and $\nu_M(^{111}\text{Cd}:\text{RNi}_2)$ in Fig. 6 shows that these quantities have a rather similar spin dependence characterized by a strong nonlinear decrease between $R=\text{Gd}$ and Dy . The Curie temperatures of RNi_2 deviate in a similar way from the de Gennes relation $T_C \propto (g-1)^2 J(J+1)$. Even quantitatively, $\Delta\nu_M$ and $\nu_M(^{111}\text{Cd}:\text{RNi}_2)/4$ —the contribution of one R neighbor to $\nu_M(^{111}\text{Cd}:\text{RNi}_2)$ —are very close to each other (e.g., 3.9 and 4.5 MHz, respectively, for $R=\text{Gd}$). Although an accidental similarity can *a priori* not be excluded, it seems possible that the nonlinearity in the spin dependence of $\Delta\nu_M$ and $\nu_M(^{111}\text{Cd}:\text{RNi}_2)$ are caused by the same mechanism. For an understanding of this mechanism, a first-principles calculation of the spin densities induced in RNi_2 by exchange with the $4f$ spins appears necessary.

When analyzing the spin dependence of the magnetic hyperfine field of ^{111}Cd in RCO_2 (Ref. 3), we have assumed (i)

that the $3d$ and the $4f$ contributions to B_{hf} have opposite signs and (ii) that the $4f$ contribution is a linear function of $(g-1)J$. Both assumptions are overruled by the present experimental data. With these results, the variation of $B_{\text{hf}}(^{111}\text{Cd}:\text{RCO}_2)$ can practically be attributed to the spin dependence of B_{hf}^{4f} (Fig. 6) alone which implies that the Co $3d$ moment is almost constant from $R=\text{Gd}$ to $R=\text{Er}$.

In summary, up to four components with different magnetic interaction frequencies ν_M^j have been detected in the PAC spectra of ^{111}Cd on R sites of $\text{R}_{1-x}\text{Y}_x\text{Co}_2$. These frequencies are to a large extent independent of the Y concentration ($x \leq 0.6$ for $R=\text{Tb}$). They are related to the number n_R of nearest R neighbors of the PAC probe by $\nu_M^j = \nu_M(4Y) + \Delta\nu_M \times n_R$. The frequency $\nu_M(4Y)$ can be identified as the contribution of the $3d$ sublattice to the magnetic hyperfine interaction. From the observation that $\nu_M(4Y)$ is independent of the Y concentration it follows that the $3d$ moment of the nearest Co environment of the probe is constant up to $x=0.6$ (in $\text{Tb}_{1-x}\text{Y}_x\text{Co}_2$). The frequency steps $\Delta\nu_M$ reflect the spin polarization directly induced by the $4f$ spins at the probe nucleus. The variation of $\Delta\nu_M$ with the $4f$ spin shows a pronounced nonlinearity which strongly resembles the $4f$ -spin dependence of the magnetic hyperfine interaction of ^{111}Cd in RNi_2 .

ACKNOWLEDGMENTS

One of the authors (A.F.P.) acknowledges financial support from AvH Foundation (Germany) and CICPBA (Argentina).

*Present address: Instituto de Magnetismo Aplicado, P.O. Box 155, 28230 Las Rozas, Madrid, Spain.

†Electronic address: forker@iskp.uni-bonn.de

¹R. G. Barnes, in *Handbook of Chemistry and Physics of Rare Earths*, edited by K. A. Gschneidner and L. Eyring (North Holland, Amsterdam, 1979), Vol. 2, Chap. 18.

²K. H. J. Buschow, in *Ferromagnetic Materials*, edited by E. P. Wohlfarth (North Holland, Amsterdam, 1980), Vol. 1, Chap. 4.

³P. de la Presa, S. Müller, A. F. Pasquevich, and M. Forker, *J. Phys.: Condens. Matter* **12**, 3423 (2000).

⁴E. Gratz and A. S. Markosyan, *J. Phys.: Condens. Matter* **13**, R385 (2001).

⁵N. H. Duc and P. E. Brommer, in *Handbook of Magnetic Materials*, edited by K. H. J. Buschow (Elsevier Science Publishing, Amsterdam, 1999), Vol. 12, p. 259.

⁶S. Hirosawa, T. Tsuchida, and Y. Nakamura, *J. Phys. Soc. Jpn.* **47**, 804 (1979).

⁷S. Hirosawa and Y. Nakamura, *J. Phys. Soc. Jpn.* **51**, 2819 (1982).

⁸S. Hirosawa and Y. Nakamura, *J. Magn. Magn. Mater.* **25**, 284 (1982).

⁹K. Yoshimura, S. Hirosawa, and Y. Nakamura, *J. Phys. Soc. Jpn.*

53, 2120 (1984).

¹⁰S. K. Arif and M. A. H. McCausland, *J. Phys. F: Met. Phys.* **5**, L247 (1975).

¹¹S. K. Arif, J. W. Ross, and M. A. H. McCausland, *Physica B & C* **86-88 B**, 158 (1977).

¹²Y. Berthier, D. Gignoux, and A. Tari, *J. Magn. Magn. Mater.* **58**, 265 (1986).

¹³H. Frauenfelder and R. M. Steffen, in *Perturbed Angular Correlations*, edited by K. Karlsson, E. Matthias, and K. Siegbahn (North Holland, Amsterdam, 1963).

¹⁴K. M. B. Alves, N. Alves, L. C. Sampaio, S. F. Da Cunha, and A. P. Guimarães, *J. Appl. Phys.* **67**, 5867 (1990).

¹⁵V. A. Vasil'kovskii, N. M. Kovtun, A. K. Kuprianov, S. A. Nikitin, and V. F. Ostrovskii, *Sov. Phys. JETP* **38**, 342 (1974).

¹⁶I. A. Campbell, *J. Phys. F: Met. Phys.* **2**, L47 (1972).

¹⁷N. V. Baranov, A. A. Yermakov, A. N. Pirogov, A. E. Teplykh, K. Inoue, and Yu. Hosokoshi, *Physica B* **269**, 284 (1999).

¹⁸D. Guenzburger, R. R. Sobral, and A. P. Guimarães, *J. Phys.: Condens. Matter* **6**, 2385 (1994).

¹⁹S. Müller, P. de la Presa, and M. Forker, *Hyperfine Interact.* (to be published).